

# A Pose Measurement Method of a Non-Cooperative Spacecraft Based on point cloud feature

Peng Li<sup>1,\*</sup>, Mao Wang<sup>2</sup>, Dong Zhou<sup>3</sup>, Wenxiao Lei<sup>4</sup>

1. Aerospace College, Harbin Institute of Technology, Harbin 150001, China  
E-mail:lipe\_123@126.com

2,3,4. Aerospace College, Harbin Institute of Technology, Harbin 150001, China

**Abstract:** This paper investigates the Attitude measurement for the Non-Cooperative Spacecraft problem. Considering there are no or few prior knowledge for the target, an autonomous measurement method for relative position and attitude of space non-cooperative spacecraft is proposed to solve the problem of relative position and attitude measurement of non-cooperative spacecraft in orbit capture in this paper. Specifically, a normal feature extraction method based on satellite plane is adopted, which can provide a good initial condition for solving the attitude matrix of the final target. The relative position and attitude of the satellite can be measured even if the rotation angle of the target is very large. Experiments show that the pose and motion method for measurement proposed in this paper has high accuracy and good stability.

**Key words:** Non-cooperative target; point cloud; Plane feature; Pose estimation

## 1 INTRODUCTION

In recent years, human space activities are increasing, and more and more spacecraft are launched every year. With the passage of time, there will be some malfunctioning spacecraft and abandoned spacecraft in many space crafts, which will seriously affect the operation safety of other spacecraft in orbit. Space target acquisition technology [1] is used for on orbit maintenance of spacecraft and cleaning of abandoned spacecraft, which has become a key research direction and research hot spot in the space field.

According to whether the space target to be captured has effective prior information, the space target can be divided into cooperative target and non-cooperative target. Among them, cooperative target acquisition technology has been relatively mature, and has been successfully applied to some spacecraft on orbit maintenance projects. E.g. ETS-VII, XSS-11, DART and Orbital Express [2]. Due to the lack of communication on the information level and the lack of cooperation in maneuvering behavior, non-cooperative targets (including no auxiliary measurement equipment such as cooperative marker and transponder installed, nor for capture and fixation The acquisition of satellites with fixed devices) such as space failure satellites [3] and space waste, is more challenging.

The service objects of space missions are generally non cooperative objects without cooperative cursor and without prior motion parameters. Therefore, as the first stage of on orbit acquisition technology of space non cooperative targets, the estimation of target motion parameters and 3D reconstruction has become an important problem to be solved urgently in the field of space technology.

Due to the non-cooperative nature of this scenario, active sensors, such as radar, Lidar, Binocular or TOF camera, are a viable alternative for sensing the target position. Newcombe et al. [4] and Izadi et al. [5] proposed Kinect

fusion and reconstruction algorithm based on depth image. In their method, the iterative nearest neighbor algorithm is used to estimate the pose transformation matrix between the frame and the model, which effectively reduces the accumulated error caused by the long track or time. The project [6] of the European Space Agency (ESA) is to capture the abandoned spacecraft through a tethered flying net or claw. In the process of capturing, laser ranging and visual measurement are used to obtain the relative pose parameters of non-cooperative targets. The United States Defense Advanced Research Projects Agency's Phoenix program [7] uses binocular stereo vision to measure the relative pose parameters of non-cooperative spacecraft in the approach phase. Japan Aerospace Development Agency [8] uses stereo vision imaging to obtain the 3D shape of non-cooperative microsatellites and the method based on 3D model matching to estimate the relative pose of the target.

In 2012, Regoli [9] et al. obtained the pose and state of the target by performing edge detection and plane fitting on the images obtained by the TOF camera, but this method needs to provide the initial pose of the target. Terui [10] and other scholars proposed a three-dimensional point cloud based on binocular camera reconstruction, Extended Kalman filter algorithm was used to predict and correct the pose parameters. But its algorithm needs to calculate a large number of feature points, which is very time-consuming. D'Amico [11] performs pose measurement based on model matching. By optimizing the initial pose estimation algorithm for target tracking, it avoids the occurrence of coarse initialization errors, and reduces the calculation amount of pose solution through algorithm optimization. He Y [12] extracts the characteristics of the target point cloud data and uses particle filtering to track the target pose effectively.

The paper is organized as follows. Section 2 presents the feature extraction process of satellite solar panels in detail, including how to use the angle between plane normal vector and principal direction. In part three, the algorithm is verified by experiments. And conclusion is drawn in the fourth part.

## 2 POSE ESTIMATION

The pose estimation framework proposed in this paper is designed to process 3-D point clouds which can be provided by LIDARs or stereovision systems. In this paper, a TOF camera [13] is used as our data acquisition equipment.

For non-cooperative targets, it will be very time-consuming to use binocular camera to obtain depth information of targets by matching feature points if some acceleration methods are not used. However, three dimensional information of the target can be obtained in real time with a TOF camera.

The first task to be executed by the system is the recognition of the target's geometrical properties. Assuming that the non-cooperative target satellite we want to measure is as shown in the figure 1. The corresponding point cloud data is as shown in the figure 2.



Fig. 1. Target satellites model



Fig. 2. The point cloud of target satellites model

As we can see from the fig. 2, in the experimental scene, there are many noise points in the acquired point cloud data, and the edge features are not easy to extract. For the non-cooperative target model adopted in this paper, the correlation characteristics of the plane of the solar array of the satellite are calculated to estimate the position and attitude of the target.

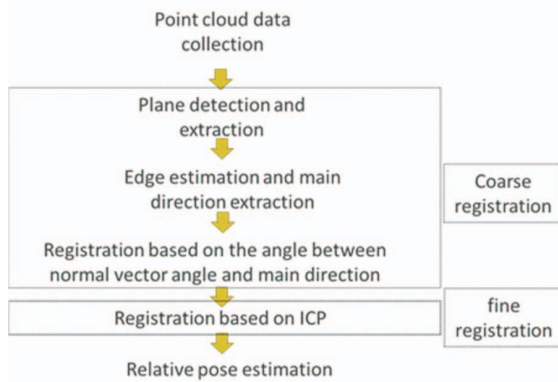


Fig.3 Flow chart of the pose estimation process

The algorithm flowchart is shown in Figure 3.

### 2.1 Plane extraction

In order to reduce the computational complexity, it is necessary to do voxel filtering on the data before plane extraction.

In this paper, Random Sample Consensus (RANSAC) [14] method is used for plane extraction. RANSAC is an iterative method, which estimates the parameters of mathematical model from the data set polluted by noise. It has the same effect as the least square method, and its application is different. RANSAC algorithm assumes that there are inner points and outer points in the data set, and only the determined inner points can be used to calculate the model, and the outer points should not have any impact on the solution of the model parameters

In this paper, the model data obtained can be treated as the data set. The points in and around the solar panel can be regarded as inner points, and the remaining points can be regarded as outer points. It is assumed that the model of inner point is conform to a plane model.

Using RANSAC algorithm to fit the target point cloud, the detailed steps are as follows:

- 1) In the original point cloud data, randomly select three points that are not collinear, and calculate the plane equation corresponding to the selected point cloud:  $Ax + By + Cz + D = 0$ ;

- 2) Calculate the distance from each point cloud to this plane  $d_i = |Ax_i + By_i + Cz_i + D|$ ;

- 3) Set the threshold value  $th$ , when  $D_i \leq th$ , the point is the internal point, and count the number of internal points  $n$ ; otherwise, it is the external point.

- 4) Repeat the above steps, iterate  $k$  times, and the plane with the most number of inner points in the region is exactly what we want.

The result shows a better plane when the value of  $th$  is set to be 0.009 m and the number of iterations times  $k$  is set to 50. The plane extracted is shown in Figure 4.

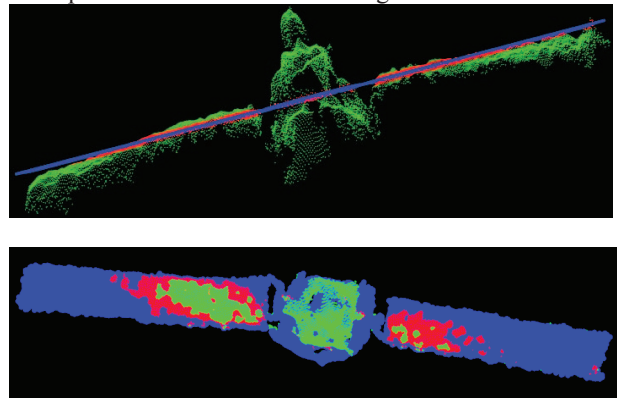


Fig.4 The result of plane extraction. The green points are origin data, the red points are inner data, the blue points are fitted plane.

### 2.2 Coarse registration by normal vector angle

After detecting the plane of solar array, it is easy to obtain the normal vector of the plane. Assuming that the normal vectors of the current frame point cloud and the next frame point cloud are  $\mathbf{n}_1, \mathbf{n}_2$ , which are two different surface vectors,  $\mathbf{n}_1$  and  $\mathbf{n}_3$  are parallel as  $\mathbf{n}_3$  is obtained by

translating  $n_1$  to make sure that the starting points of  $n_2$  and  $n_3$  are the same. That is,  $n_2$  and  $n_3$  are coplanar.

The normal angle between  $n_2$  and  $n_3$  can be expressed as the following:

$$\theta = \arccos \left( \frac{\mathbf{n}_2 \cdot \mathbf{n}_3}{|\mathbf{n}_2||\mathbf{n}_3|} \right) \quad (1)$$

Where the value range of  $\theta$  is  $[0, \pi]$ .

Unit rotate axis  $\mathbf{r}$  can be obtained by equation 2,  $\mathbf{r}$  is perpendicular to  $n_2$  and  $n_3$ .

$$\mathbf{r} = \frac{\mathbf{n}_2 \times \mathbf{n}_3}{|\mathbf{n}_2 \times \mathbf{n}_3|} \quad (2)$$

Where  $\times$  means cross product.

After obtaining the rotation vector and the rotation angle, the rotation matrix can be further obtained.

In order to write the expression of rotation by the axis  $\mathbf{r}$  in the form of matrix, the matrix form of cross product is as follows:

$$\mathbf{M} = \begin{bmatrix} 0 & -r_z & r_y \\ r_z & 0 & -r_x \\ -r_y & r_x & 0 \end{bmatrix} \quad (3)$$

The transformation of Rodriguez's rotation formula can be written in matrix form.

$$R(\mathbf{r}, \theta) = \mathbf{I} + \sin \theta \mathbf{M} + (1 - \cos \theta) \mathbf{M}^2 \quad (4)$$

After expansion, the rotation matrix  $R$  can be expressed as follows:

$$R = \begin{bmatrix} \cos \theta + r_x^2 (1 - \cos \theta) & -\sin \theta r_z + (1 - \cos \theta) r_x r_y \\ \sin \theta r_z + (1 - \cos \theta) r_x r_y & \cos \theta + r_y^2 (1 - \cos \theta) \\ -\sin \theta r_y + (1 - \cos \theta) r_x r_z & \sin \theta r_x + (1 - \cos \theta) r_y r_z \\ \sin \theta r_y + (1 - \cos \theta) r_x r_z \\ -\sin \theta r_x + (1 - \cos \theta) r_y r_z \\ \cos \theta + r_z^2 (1 - \cos \theta) \end{bmatrix} \quad (5)$$

After a translation by the two plane centroids, plane 1 can be transformed to be plane 3, as shown in the Figure 4.

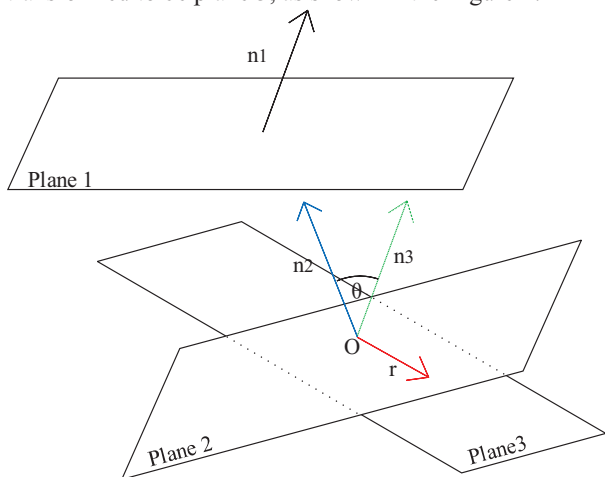


Fig.5 Schematic diagram of coarse registration by the plane normal vector. O is the center of plane 2.

In this way, two targets with far initial positions are transformed to the same plane, which is convenient for angle calculation in the next stage.

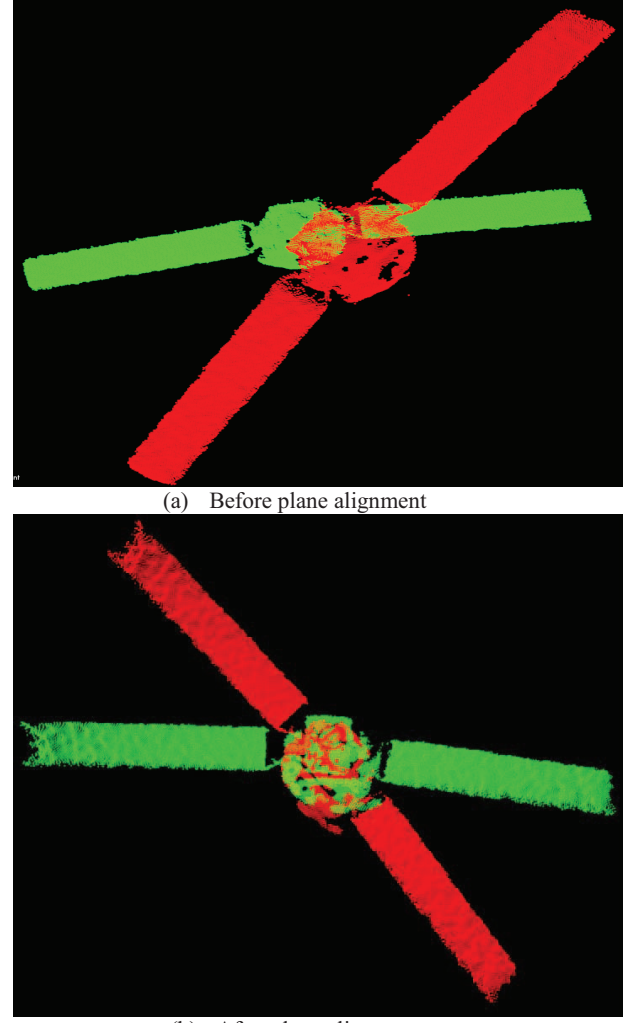


Fig.6 Coarse registration by the plane normal vector. The red one is the current frame and the green one is the next frame.

### 2.3 Edge estimation and main direction extraction

After obtaining the plane where the solar panel of the satellite is located, the smallest circumscribed rectangle containing the solar panel can be further fitted. Principal component analysis [16] is used to obtain the principal direction of rectangular plane.

With the coordinates of data points, the covariance matrix  $A$  can be obtained by equation 6.

$$\text{cov}(X_i, X_j) = E[(X_i - \mu_i)(X_j - \mu_j)] \quad (6)$$

$$A = \begin{bmatrix} \text{cov}(x, x) & \text{cov}(x, y) & \text{cov}(x, z) \\ \text{cov}(x, y) & \text{cov}(y, y) & \text{cov}(y, z) \\ \text{cov}(x, z) & \text{cov}(y, z) & \text{cov}(z, z) \end{bmatrix} \quad (7)$$

In order to distribute all points uniformly along the coordinate axis, the covariance matrix needs to be transformed into a diagonal matrix.

$$A = U \Sigma V^* \quad (8)$$

$\Sigma$  is a diagonal matrix and feature vectors are represented as follows:

$$V^* = [\epsilon'_1 \quad \epsilon'_2 \quad \epsilon'_3] \quad (9)$$

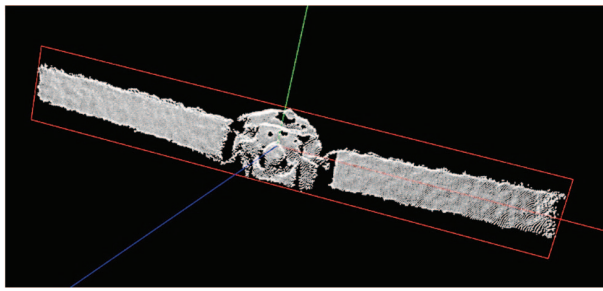


Fig.7 The red box is the extracted rectangular box, the direction of the red line is the main direction of the plane

$$\Sigma = \begin{bmatrix} \lambda_1 & 0 & 0 \\ 0 & \lambda_2 & 0 \\ 0 & 0 & \lambda_3 \end{bmatrix} \quad (10)$$

Assuming that  $\lambda_1 > \lambda_2 > \lambda_3$ , The column vector corresponding to  $\lambda_1$  is the main direction. Using the obtained vector as the direction corresponding to the natural axis of the object, the maximum and minimum positions of the points on the plane along the X, Y, and Z directions can be calculated by projecting the original data to the new coordinate axis. Based on these maximum and minimum values, the position of the rectangular frame can be easily constructed, as we can see from the figure 7 in this way.,

#### 2.4 fine registration

Generally speaking, the target satellite is treated as a rigid body, and it is assumed that no deformation occurs during the data acquisition process. For the two adjacent three-dimensional point clouds  $C_i$  and  $C_{i+1}$ , the relative positions between the two will be very close because the rough normal registration has been performed using the plane normal vector and the main direction before. Therefore, in the fine registration phase, this paper directly uses ICP [15] algorithm to register it.

The ICP procedure typically comprises several different phases for each of which many variants have been derived.

Among them, the steps that must be performed include corresponding point matching, selection of error metric functions, and minimization of error functions.

Using  $T_i = [R_i, t_i]$  to express the position and attitude transformation relationship between  $C_i$  and  $C_{i+1}$ .

$$p_j^{(i+1)} = R_i p_j^{(i)} + t_i \quad (11)$$

$$\text{s.t. } R^T R = I_{3 \times 3}, \det(R) = 1$$

An error function is defined as shown in Eq. (2), i.e., finding the best transformation matrix  $T$  by minimizing the mean squared distance of the corresponding points between the two point clouds.

$$E = \min \frac{1}{N_p} \sum_{i=1}^{N_p} \|p_j^{i+1} - q_j^{i+1}\|^2 \quad (12)$$

$\|\cdot\|^2$  denotes L<sub>2</sub> norm.

Rotation matrix  $R$  can be solved by singular value

decomposition(SVD).The centroid of the point cloud in the current frame and the next frame can be expressed as:

$$\mu_p = \frac{1}{N_p} \sum_{i=1}^{N_p} p_i \quad (13)$$

$$\mu_q = \frac{1}{N_q} \sum_{i=1}^{N_q} q_i \quad (14)$$

Compute the optimal translation  $t$  as:

$$t = \mu_q - R \mu_p \quad (15)$$

Although the ICP algorithm has good performances for the rigid registration, It does not get the correct registration results if the initial positions of the two point clouds to be registered are not significantly different. Otherwise, it is easy to fall into a local optimum and not obtain accurate results.

### 3 EXPERIMENTAL RESULTS

In order to verify the effectiveness of the non-cooperative target pose measurement method of a non-cooperative GEO spacecraft based on point cloud feature. The ToF Camera used in the experiment is a ODOS Swift camera, whose specifications are given in Table 1.

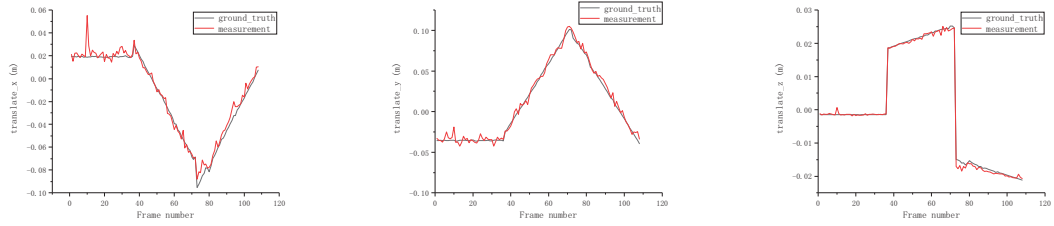
Table 1. ODOS Swift camera specifications.

Parameter	Value
Sensor size	640 px*480 px
range	0.5m-6m
Field of view	47°-37°
focal length	5mm

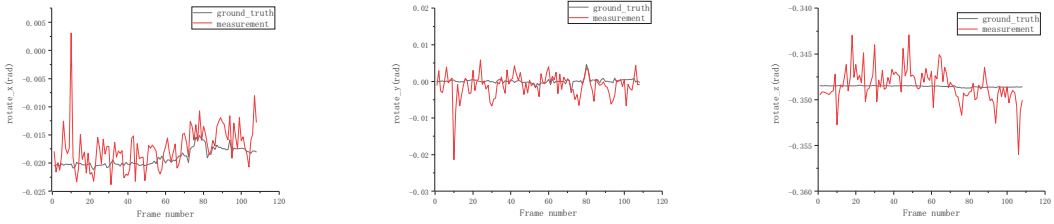
In order to get more accurate motion state of real object, a program is used to simulate the motion and rolling state of the object, so that it is easy to get the true value of the target motion related parameters, and the experiment is completed by combining the actual point cloud data of satellite model with simulation.



Fig.8 Schematic diagram of satellite movement



(a) The result of translation vector estimation



(b) The result of rotation angle estimation

Fig.9 pose estimate output, attitude given in Euler angles (rad), compared to the true values.

In the simulation of the target motion state, rotating and translating the point cloud simultaneously, The satellite spins first, then moves as it rotates, we assumed  $\omega_x=0.1$  rad/s,  $\omega_y=0.1$  rad/s,  $\omega_z=0.2$  rad/s.  $v_{tx}=0.1$ m/s,  $v_{ty}=0.1$ m/s,  $v_{tz}=0.1$ m/s. Due to the acquired point cloud data of satellite model already contains noise, the data is no longer processed with noise.

Figure 8 shows the schematic diagram of the initial pose of the target and the motion state afterwards. By measuring the pose transformation relationship between two adjacent point cloud images, and comparing it with the true value, we can obtain the figure 9 ,

It can be seen from the figure 9 that the non-cooperative target pose measurement algorithm based on point cloud feature can be used to estimate non-cooperative satellite accurately.

Table 2. Analysis and statistics of measurement error

	Mean	standard deviation
rotation_error_x (rad)	-0.0018	0.00324
rotation_error_y (rad)	0.00117	0.00329
rotation_error_z (rad)	-0.00012	0.0018
translation_error_x (m)	-0.00242	0.00515
translation_error_y (m)	-0.00178	0.00412
translation_error_z (m)	0.00024	0.00065

It can be seen from table 2 that the error in X direction is the largest among the three directions. The maximum error of rotation angle is about  $0.1^\circ$ , and the maximum translation error is not more than 2.5 mm. Considering the actual size of the model is about  $700\text{mm} \times 200\text{mm} \times 200\text{mm}$  , the minimum distance between the target and the camera is greater than 1.2 m,

Compared with reference [17], the measurement error of the target satellite with the size of  $300\text{ mm} \times 250\text{ mm} \times 200$

mm is not less than  $8^\circ$  at 1.8 m. Therefore, the non-cooperative pose estimation method based on the plane characteristics of point cloud in this paper is more accurate than that in reference [17].

## 4 CONCLUSION

Close-range relative pose measurement of non-cooperative targets in space is one of the key technologies for on-orbit services. In this paper, a method for non-cooperative target pose measurement based on point cloud feature is proposed and verified by several experiments. Experimental results show that the proposed method can be used to effectively identify the features of non-cooperative targets and measure the relative pose of the target. However, this method takes a lot of time to accurately extract the plane. Therefore, the focus of future research will be how to improve the speed of the algorithm by feature extraction with less time.

## ACKNOWLEDGMENTS

This work was supported in part by the National Key R&D Program of China (No. 2019YFB1312001).

## REFERENCES

- [1] Christian J A, Cryan S. A survey of LIDAR technology and its use in spacecraft relative navigation[C]//AIAA Guidance, Navigation, and Control (GNC) Conference. 2013: 4641.
- [2] Woffinden D C, Geller D K. Navigating the road to autonomous orbital rendezvous[J]. Journal of Spacecraft and Rockets, 2007, 44(4): 898-909.
- [3] Sullivan B R, Akin D L. A survey of serviceable spacecraft failures[J]. Databases, 2001, 1(4540).

- [4] Newcombe R A, Izadi S, Hilliges O, et al. Kinectfusion: Real-time dense surface mapping and tracking[C]//ISMAR. 2011, 11(2011): 127-136.
- [5] Izadi S, Kim D, Hilliges O, et al. KinectFusion: real-time 3D reconstruction and interaction using a moving depth camera[C]//Proceedings of the 24th annual ACM symposium on User interface software and technology. ACM, 2011: 559-568.
- [6] Bischof. ROGER-Robotic geostationary orbit restorer[C] //54th International Astronautical Congress of the International Astronautical Federation, the International Academy of Astronautics, and the International Institute of Space Law. 2003: IAA. 5.2. 08.
- [7] Kimura S, Nagai Y, Yamamoto H, et al. Approach for on-orbit maintenance and experiment plan using 150kg-class satellites[C]//2005 IEEE Aerospace Conference. IEEE, 2005: 837-845.
- [8] Terui F, Kamimura H, Nishida S. Motion estimation to a failed satellite on orbit using stereo vision and 3D model matching[C]//2006 9th International Conference on Control, Automation, Robotics and Vision. IEEE, 2006: 1-8.
- [9] Regoli L, Ravandoor K, Schmidt M, et al. Advanced techniques for spacecraft motion estimation using PMD sensors[J]. IFAC Proceedings Volumes, 2012, 45(4): 320-325.
- [10] Terui F, Kamimura H, Nishida S. Motion estimation to a failed satellite on orbit using stereo vision and 3D model matching[C]//2006 9th International Conference on Control, Automation, Robotics and Vision. IEEE, 2006: 1-8.
- [11] D'Amico S, Benn M, Jørgensen J L. Pose estimation of an uncooperative spacecraft from actual space imagery[C]//5th International Conference on Spacecraft Formation Flying Missions and Technologies. 2013.
- [12] He Y, Liang B, He J, et al. Non-cooperative spacecraft pose tracking based on point cloud feature[J]. Acta Astronautica, 2017, 139: 213-221.
- [13] Foix S, Alenya G, Torras C. Lock-in time-of-flight (ToF) cameras: A survey[J]. IEEE Sensors Journal, 2011, 11(9): 1917-1926.
- [14] Fischler M A, Bolles R C. Random sample consensus: a paradigm for model fitting with applications to image analysis and automated cartography[J]. Communications of the ACM, 1981, 24(6): 381-395.
- [15] Besl P J, McKay N D. Method for registration of 3-D shapes[C]//Sensor fusion IV: control paradigms and data structures. International Society for Optics and Photonics, 1992, 1611: 586-606.
- [16] Pearson K. LIII. On lines and planes of closest fit to systems of points in space[J]. The London, Edinburgh, and Dublin Philosophical Magazine and Journal of Science, 1901, 2(11): 559-572.
- [17] Terui F, Kamimura H, Nishida S. Motion estimation to a failed satellite on orbit using stereo vision and 3D model matching[C]//2006 9th International Conference on Control, Automation, Robotics and Vision. IEEE, 2006: 1-8.